

EFFECT OF FIBER ORIENTATION ON THE DELAMINATION BEHAVIOUR OF GLASS-CARBON HYBRID INTERFACE

AROCKIA JULIAS. A¹, RAJARAMAN. R² & VELA MURALI³

¹Department of Mechanical Engineering, BSA Crescent Institute of Science & Technology, Chennai, India

²Department of Mechanical Engineering, SRM Institute of Science & Technology, Vadapalani campus, Chennai, India

³Department of Mechanical Engineering, CEG campus, Anna University, Chennai, India

ABSTRACT

The delamination behavior of glass-carbon hybrid laminate with glass and carbon fiber on either side of the mid-plane was studied using double cantilever beam test. The stacking sequence and fiber orientation of the hybrid laminate was taken as $[G_0/G_{135}/G_{90}/G_{45}/C/C//G/G/G_{45}/G_{90}/G_{135}/G_0]$. Three different laminates were obtained by changing the fiber orientation of the mid-layers as C/C//G/G. Laminates were prepared by hand lay-up technique and post cured by compression. The test was conducted as per ASTM standard D5528. The strain energy release rate G_{Ic} calculated using modified beam theory method was found to be higher for the laminate with mid-layers as C_{90}/G_0 in comparison with that of the other two laminates. Fractographic analysis of the delaminated surfaces using scanning electron microscope indicates hackles, striations and fiber fracture. Hackles that provides more resistance to crack propagation leading to increase in inter laminar fracture toughness are observed in the glass fiber side of the specimen with C_{90}/G_0 interface.

KEYWORDS: Glass, Carbon, Hybrid, Delamination & Fracture

Received: Apr 27, 2018; **Accepted:** May 23, 2018; **Published:** Jun 20, 2018; **Paper Id.:** IJMPERDJUN2018120

INTRODUCTION

In structural applications Fiber Reinforced Polymer (FRP) composites are used in the form of laminates. These layered composites are fabricated by binding multiple layers together. They suffer from delamination failure due to poor inter laminar fracture toughness. The effect of delamination will further increase when the adjacent layers are stacked with different fiber type. In hybrid laminates stacked with carbon/glass fiber the specimens failed by brittle cracking, crack growth in waves and large displacement [1]. Inter laminar fracture toughness was found to be higher for the inter-ply hybrid composites in comparison with that of the single-fiber composites. The crack growth was dominated by Mode I fracture [2]. Double Cantilever Beam (DCB) test was found to be a viable method to measure the interlaminar mode I fracture resistance. In DCB test the opening displacement between two DCB arms, reaction force at the pulling point and the delamination crack length can be obtained [3]. The critical strain energy release rate (G_{Ic}) calculated using these data indicate the resistive force required to create two new surfaces [4].

In carbon-epoxy laminates G_{Ic} was found to be better for the specimens with $0^\circ/90^\circ$ interface when compared to that of the specimens with $0^\circ/0^\circ$ interface at the mid-plane. But, the delamination migrates towards the neighboring layers by extending in the transverse direction [5]. This phenomenon of crack migrating from one lamina to an adjacent lamina may deviate the result from true fracture toughness value [6]. In carbon-epoxy laminates with $0^\circ/0^\circ$ fiber orientation at the mid-plane, fiber bridging occurred. This increased with increase in θ

and was found to be maximum for the specimen with $0^\circ//90^\circ$ interface at the mid-plane [7]. The interlaminar fracture toughness of glass-epoxy was also found to be higher for the specimen with $0^\circ//90^\circ$ interface at the mid-plane [8]. In multidirectional FRP laminates, the fracture toughness depends on both the amount of fiber bridging and the interface angles [9].

Fractographic study using Scanning Electron Microscope (SEM) on the new surfaces generated due to mode I fracture shows resin rich regions in glass fiber laminate and brittle fracture in carbon fiber laminate [10]. Further analysis on the delaminated surfaces shows, fiber pull-out with few cusps in the case of carbon-epoxy [11] and broken fiber pulled-out from the resin and scarps with opposing faces in glass-epoxy laminates [12]. However, detailed examination of fracture surfaces reveals that matrix cleavage is the main contributor to the fracture toughness under mode I loading [6].

Even though, numerous studies have been carried out on carbon-epoxy and glass-epoxy composites independently, more information about the fracture behavior of carbon-glass hybrid interface is required for designing structural components.

MATERIALS AND METHOD

In this work, DCB test was carried out by reinforcing glass and carbon fiber on either side of the delamination in the mid-plane to find the inter laminar fracture toughness between hybrid fiber layers. The layer configuration of the 12 ply laminate was taken as $[G_0/G_{135}/G_{90}/G_{45}/C/C//G/G/G_{45}/G_{90}/G_{135}/G_0]$ by stacking the quasi-isotropic glass fiber layers outside. Fiber orientation of the four layers $C/C//G/G$ near the mid-plane was varied as $C_{90}/C_0//G_0/G_{90}$, $C_{90}/C_0//G_{90}/G_0$ and $C_0/C_{90}/G_0/G_{90}$ to form three different laminates.

The hybrid FRP laminates were fabricated using 400 gsm unidirectional glass fiber and 300 gsm unidirectional carbon fiber layers. Epoxy resin (Araldite LY556) was used as matrix material with HY951 as hardener. The mixing ratio for resin-to-hardener was taken as 10:1 weight percentage to initiate the chemical reaction. The laminates were manufactured by hand lay-up technique in an open mold by stacking the fiber layers one-by-one. They were partially cured in atmospheric condition for 4 hours followed by compression in a compression molding machine for 10 minutes at 70°C under a constant pressure of 8 bar [13].

The DCB test was conducted as per ASTM standard D5528. The delamination (pre-crack) in the mid-plane was created by inserting a $100\ \mu\text{m}$ thick Teflon film at one end of the laminate [4]. The specimen length was taken as 160 mm including the pre-crack length of 70 mm at one end. The width and thickness of the specimen was taken as 25 mm and 4 mm respectively. A schematic representation of the DCB specimen is shown in Figure 1.

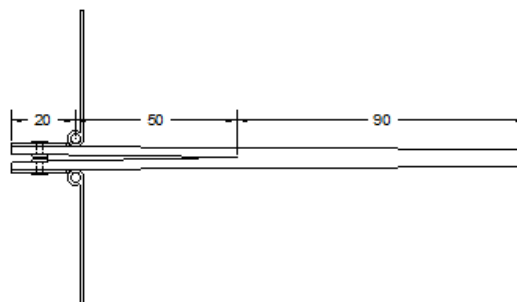


Figure 1: Schematic Representation of DCB Specimen

The Loading hinges used to transfer the load from UTM to the specimen was riveted carefully after drilling two holes of 2 mm diameter in the specimen. The sides of the specimens were marked at an equal interval of 5 mm from the crack tip. The end of the hinges are clamped to the vice of the UTM and loaded as shown in Figure 2. The test was conducted at a constant speed of 2 mm/min. The crack extension was monitored through a 12.1 megapixel optical camera with 20X optical zoom. The load and displacement values corresponding to each 5 mm crack extension was manually recorded by visual inspection. Five samples were tested for each type and the load-displacement value taken at each interval is used to calculate the Mode I strain energy release rate (G_{Ic}).



Figure 2: DCB Specimen Being Tested at UTM

Modified Beam Theory (MBT) method given in Equation (1) is preferred over other methods to find the G_{Ic} [2]. In this equation, P is the applied load in N, δ is the load point displacement in mm, b is the width of the specimen in mm, a is the delamination length in mm and Δ is the correction factor in mm. The correction factor Δ was found by plotting the cube root of compliance against the crack length and measuring the deviation in the x intercept as shown in Figure 3. Compliance C is the ratio of load point deflection (δ) and applied load (P).

$$G_{Ic} = \frac{3P\delta}{2b(a + |\Delta|)} \quad (1)$$

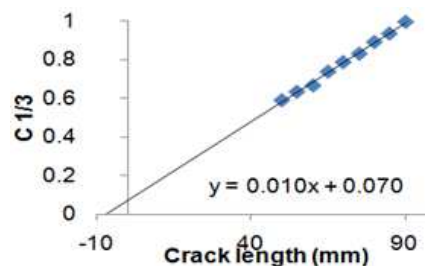


Figure 3: Determination of Rotation Correction Factor Δ

RESULTS AND DISCUSSIONS

Three different laminates with glass-carbon interface at the mid-plane were tested by changing the fiber orientation of the layers on either side of the delamination. The load-displacement curve obtained is shown in Figure 4. The curve is found to be similar for the specimens with C_0/G_{90} interface and C_{90}/G_0 interface. Whereas, the displacement at crack initiation is found to be more for the specimen with C_{90}/G_0 interface. The maximum load taken by these two specimens are about 10 N more in comparison to that of the specimen with C_0/G_0 interface.

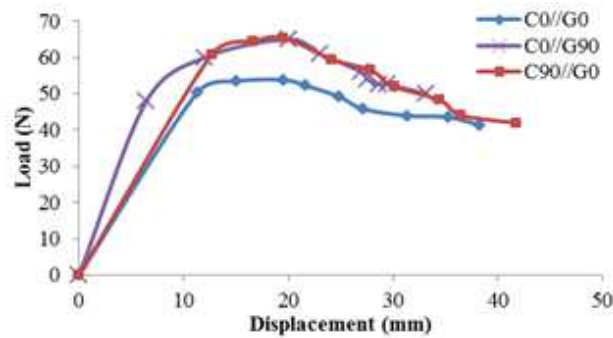


Figure 4: Load – Displacement Curve

During the test, it was observed that the crack propagate quickly along the 0° oriented unidirectional fibers for the specimen with $C_0//G_0$ interface. Carbon fiber particles were also deposited on the glass fiber layer as shown in Figure 5 (a). In the specimen with $C_0//G_{90}$ interface, crack jumping from the 90° oriented glass fiber layer into the adjacent layer was observed as shown in Figure 5 (b). This reduced the thickness of the beam on one side leading to increase in deflection due to unsymmetrical bending. Similar crack jumping was also reported in earlier studies [5]. In the specimen with $C_{90}//G_0$ interface, fiber bridging occurred as shown in Figure 5 (c). This is due to the 90° oriented carbon fiber strand that sticks to the glass fiber layer and starts separating the fibers within the carbon fiber strand on either side with respect to its axis. The bridging of fiber between the two sides of the crack plane increases the delamination resistance [7].

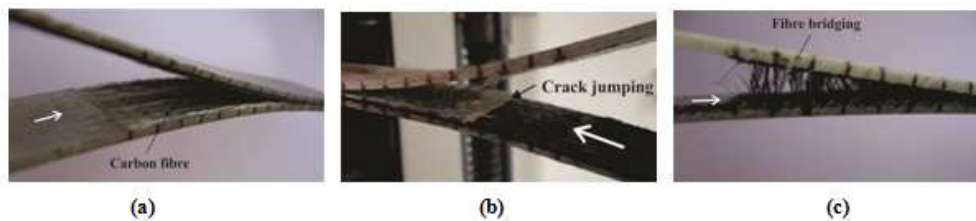


Figure 5: Delaminated Specimens
(a) $C_0//G_0$ Interface (b) $C_0//G_{90}$ Interface (c) $C_{90}//G_0$ Interface

The mode I strain energy release rate G_{Ic} calculated using modified beam theory method and the resistance curve plotted between G_{Ic} and crack length is shown in Figure 6. From the graph it is inferred that the G_{Ic} value corresponding to crack initiation at pre-crack region is higher for the specimen with $C_{90}//G_0$ interface (0.8 kJ/m^2) due to fiber bridging. This is nearly twice of that of the specimen with $C_0//G_{90}$ interface (0.4 kJ/m^2). But, the resistance curves for both the specimens are nearly same after it extends beyond 60 mm. The G_{Ic} value for the specimen with $C_0//G_0$ interface is found to be less in comparison with that of the other two specimens.

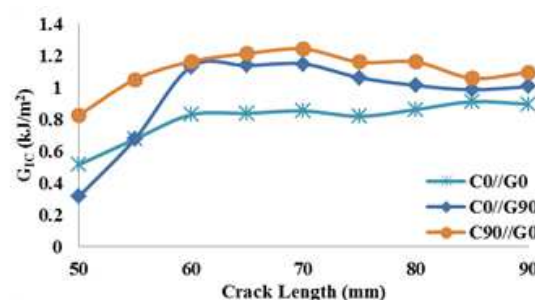
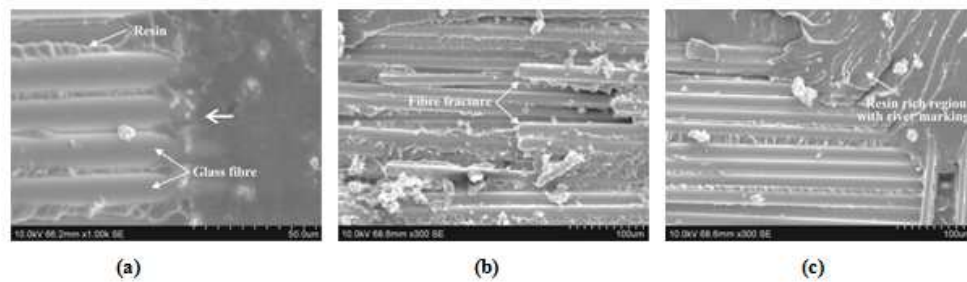


Figure 6: Resistance Curve

Fractographic Observations

In DCB test when the specimen was pulled by the UTM, the crack propagates along the mid-plane or migrating to adjacent layers and separate laminate by creating two new surfaces. By visually inspecting these surfaces, macro level information like crack jumping and fiber bridging can be obtained. But micro level analysis using SEM is required to understand the mechanism of failure in detail [6]. Hence, the fracture surface of the DCB specimen was examined using Hitachi S-3400 scanning electron microscope. The SEM image taken from the specimen with $C_0//G_0$ interface at the crack initiation region is shown in Figure 7 (a). Hackles were observed in the resin between the fibers. The fracture surface indicates good bonding strength between the fiber and matrix. The fiber breakage found on the glass fiber side and the resin rich region with river markings found on the carbon fiber side are shown in Figure 7 (b) and (c) respectively. The river markings (striations) are an indication of good matrix strength [9]. From these SEM images it is inferred that the matrix provides good bonding between the glass fiber and carbon fiber. The bare and flat fracture surface indicate that the crack could have propagated easily along the periphery of the 0° oriented fibers without giving much scope for the matrix to resist.



**Figure 7: SEM Images of Hybrid Laminates with $C_0//G_0$ Interface
(a) & (b) Glass Fiber Side (c) Carbon Fiber Side**

The SEM images taken near the crack tip in the glass fiber side of the specimen with $C_0//G_{90}$ interface is shown in Figure 8 (a). The fracture surface is not flat as observed in the case of $C_0//G_0$ interface. A 90° oriented glass fiber is peeled-off and separated from the matrix indicating a possible initiation of fiber bridging. The region where crack jumping occurred from the 90° oriented glass fiber layer into the adjacent layer is shown in Figure 8 (b). The glass fiber layer has been pulled-out completely and the matrix is cracked along the width direction. The resin rich region with striations observed in the carbon fiber side of this specimen is shown in Figure 8 (c). Imprints of fiber layer being pulled-out from the matrix is also visible in the carbon fiber side. This indicates good bonding strength between the fiber and resin. From the SEM images it is inferred that the glass fibers oriented at 90° in the crack plane could have started bridging and peeled-off leaving the matrix to break.

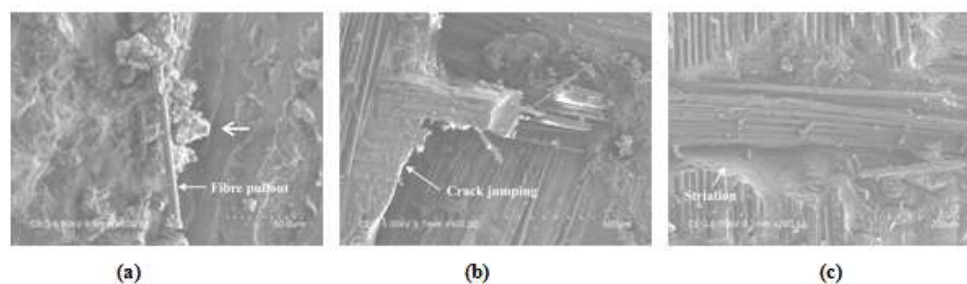


**Figure 8: SEM Images of Hybrid Laminates with $C_0//G_{90}$ Interface
(a) & (b) Glass Fiber Side (c) Carbon Fiber Side**

The SEM images taken from the glass fiber side on the specimen with C_{90}/G_0 interface is shown in Figure 9 (a). The 0° oriented glass fiber layer is not visible on the glass fiber side. Instead, the imprints of 90° oriented carbon fiber layer alone are visible. This clearly indicates that the crack has not propagated like a conventional mode I fracture. Development of two new surfaces occurs through pure fiber bridging. Hackles and fiber imprints observed indicate good bonding between the fiber and matrix. The SEM image taken at the initial crack propagation region on the carbon fiber side is shown in Figure 9 (b). The difference in depth between the pre-crack region and the fracture surface indicates that a bundle of 90° oriented carbon fiber is pulled-out and bridged. The region where imprints of 0° oriented glass fiber layer and 90° oriented carbon fiber bundle pull-out observed on the carbon fiber side is shown in Figure 9 (c). From the SEM images of this specimen it is inferred that fiber bridging will be dominating when the crack propagate along a 90° oriented unidirectional carbon fiber layer.

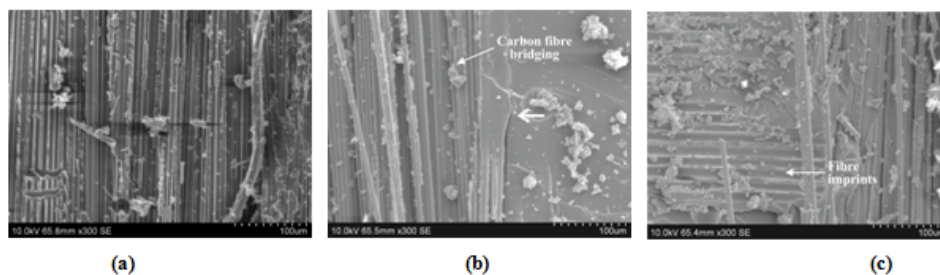


Figure 9: SEM Images of Hybrid Laminates with C_{90}/G_0 Interface
(a) Glass Fiber Side (b) & (c) Carbon Fiber Side

CONCLUSIONS

The Mode I inter laminar fracture behavior between glass and carbon fiber layer was studied by changing the fiber orientation of the mid-layers on either side of the delamination plane and the following conclusions have been made.

- Fiber bridging occurred in the specimen with C_{90}/G_0 interface due to the 90° oriented carbon fiber strand that stick to the glass fiber layer and starts separating the fibers from its strand.
- The strain energy release rate G_{Ic} at crack initiation was found to be nearly 50% higher for the specimen with C_{90}/G_0 interface but it was similar to that of C_0/G_{90} after it reaches 10 mm.
- The crack can propagate easily along the fiber surface when the fiber direction is same as that of the crack propagation direction.
- Fracture surface of the specimen with C_{90}/G_0 interface shows hackles and fiber pull-out that provide more resistance to crack propagation.

REFERENCES

1. X. Y Zhu, Z. X. Li and Y. X. Jin, *Laminar fracture behaviour of (carbon/glass) hybrid fiber reinforced laminates-I. Laminar fracture process*, *Engineering Fracture Mechanics* 44, 545-552 (1993).
2. S. F. Hwang and B. C. Shen, *Opening-mode interlaminar fracture toughness of interply hybrid composite materials*, *Composite science and Technology* 59, 1861-1869(1999).
3. S. G. Kravchenko, O. G. Kravchenko, L. A. Carlsson, R. Byron Pipes, *Influence of through-thickness reinforcement aspect ratio on mode I delamination fracture resistance*, *Composite. Structures* 125, 13–22 (2015).

4. J. I. Lim, K. Y. Rhee, H. J. Kim, D. H. Jung, *Effect of stacking sequence on the flexural and fracture properties of carbon/basalt/epoxy hybrid composites*, *Carbon Letters* 15, 125-128 (2014).
5. A. B. de Moraes, M. F. de Moura, A. T. Marques and P. T. de Castro, *Mode-I interlaminar fracture of carbon/epoxy cross-ply composites* *Composite Science and Technology*. 62, 679-686(2002).
6. E. S. Greenhalgh, C. Rogers, P. Robinson, *Fractographic observations on delamination growth and the subsequent migration through the laminate*. *Composite Science and Technology* 69, 2345-2351 (2009).
7. A. B. de Pereira and A. B. de Moraes, *Mode I interlaminar fracture of carbon/epoxy multidirectional laminates*, *Composite Science and Technology* 64, 2261-2270 (2004).
8. M. R. Shetty, K. R. Vijay Kumar, S. Sudhir, P. Raghu, A. D. Madhuranath and R. M. V. G. K. Rao, *Effect of fiber orientation on mode-I interlaminar fracture toughness of glass epoxy composites*, *Journal of Reinforced Plastics and Composite* 19, 606-620 (2000).
9. T. A. Sebaey, N. Blanco, *JOURNAL* Costa, C. S. Lopes, *Characterization of crack propagation in mode I delamination of multidirectional CFRP laminates*, *Composite Science and Technology* 72, 1251-1256 (2012).
10. R. Zenasni, A. S. Bachir, A. Arguelles, M. A. Castrillo, J. Vina, *Fracture characterization of woven fabric reinforced thermoplastic composites*, *Journal of Engineering Materials and Technology*, 129, 190-193 (2007).
11. M. D. Gilchrist and N. Svensson, *A fractographic analysis of delamination within multidirectional carbon epoxy laminates*, *Composite Science and Technology* 55, 195-207 (1995).
12. R. Marat-Mendes and M. de Freitas, *Fractographic analysis of delamination in glass epoxy composite*, *Journal of Composite Materials* 47, 1437-1448 (2013).
13. A. Arockia Julias, Vela Murali, *Effect of Carbon Fiber Position on the Impact Behavior of Glass/Carbon Fiber Hybrid Composite Laminates*, *International Journal of Applied Engineering Research*. 9, 9103-9106 (2014).

